Synthesis and Spectroscopy or Poly(9,9-dioctylfluorene-2,7-diyl-co-2,8-dihexyldibenzothiophene-S,S-dio xide-3,7-diyl)s: Solution-Processable, Deep-Blue Emitters with a High Triplet...

6 AUTHORS, INCLUDING:

Andy Monkman
Durham University

Synthesis and Spectroscopy of Poly(9,9-dioctylfluorene-2,7-diyl-*co*-2,8-dihexyldibenzothiophene-*S,S*-dioxide-3,7-diyl)s: Solution-Processable, Deep-Blue Emitters with a High Triplet Energy

**Kiran T. Kamtekar,[†] Helen L. Vaughan,[‡] Benjamin P. Lyons,[‡] Andrew P. Monkman,[‡]
Shashi U. Pandya,[§] and Martin R. Bryce*,[§]**

[†]*Zumtobel LED Division, Green Lane Industrial Estate, Spennymoor, Durham, DL16 6HL, U.K.,* [‡]*Department of Physics, Durham University, South Road, Durham, DH1 3LE, U.K., and* [§]*Department of Chemistry, Durham University, South Road, Durham, DH1 3LE, U.K.*

ABSTRACT: Poly(9,9-dioctylfluorene-2,7-diyl-*co*-2,8-dihexyldibenzothiophene-*S,S*-dioxide-3,7-diyl) copolymers (pF-S_6 **8–10**) of varying composition have been synthesized by Suzuki–Miyaura polymerization. The hexyl substituents on the dibenzothiophene-*S,S*-dioxide (S) units improve the solubility of the copolymers and increase the dihedral angles in the backbone; this shifts the emission deep into the blue (λ_{max} 420 nm for films of **10**) and increases the photoluminescence quantum yield compared with previous pF-S copolymers containing non-alkylated S units. The backbone twist restricts formation of the intramolecular charge transfer (ICT) state for low incorporation ratios of S_6 units. The triplet energy of these new copolymers increases as the percentage of the S_6 unit increases (i.e., 15, 30, 50%: **8 → 9 → 10**). The alternating copolymer **10** has a sufficiently high triplet energy (E_T 2.46 eV for onset of phosphorescence) to host a green phosphorescent iridium guest emitter, as demonstrated in electroluminescence studies which showed emission exclusively from the guest complex.
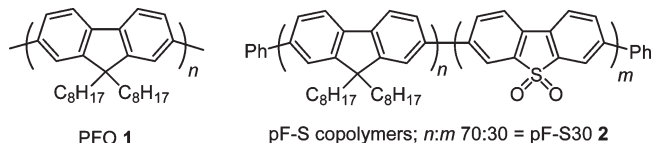
Introduction

Poly(9,9-dialkylfluorene-2,7-diyl)s, e.g. PFO **1** (Chart 1), are established as a prominent family of materials in electroluminescent devices.[1] They possess many desirable properties, namely, blue emission, high charge-carrier mobilities, good thermal and electrochemical stability, high photoluminescence quantum yields (PLQY), and facile chemical modification. A wide range of fluorene-based copolymers have been synthesized, and their optoelectronic properties have been evaluated.[2] For example, the conjugation pathway has been interrupted by copolymerization with 9,9-dihexylfluorene-3,6-diyl units.[3] Intramolecular charge transfer (ICT) interactions between donor and acceptor moieties in the main chain have been studied, although the details of these processes and the factors which allow the formation of the ICT state remain to be fully elucidated.[4]

In this context, dibenzothiophene-*S,S*-dioxide-3,7-diyl (S) is an interesting acceptor unit which is topologically similar to fluorene. Our group[5] and other workers[6] have recently incorporated S units into 9,9-dialkylfluorene (F) backbones, e.g. pF-S copolymer **2** (Chart 1). The sulfone group lowers the LUMO energy which improves electron injection. Enhanced spectral stability is also observed: green fluorenone emission, which is often a problem with fluorene-containing polymers,[7] was not detected in copolymer **2** or in model F–S co-oligomers. The emission of pF-S is red-shifted in thin films and polar solvents compared to homopoly(9,9-dialkylfluorene) for all the F:S ratios studied (*n:m* = 0.98:0.02–0.70:0.30). This is a consequence of dual emission from a polyfluorene-like local exciton (LE) state and from a lower energy ICT state which is stabilized by the S units.[8]

Chart 1
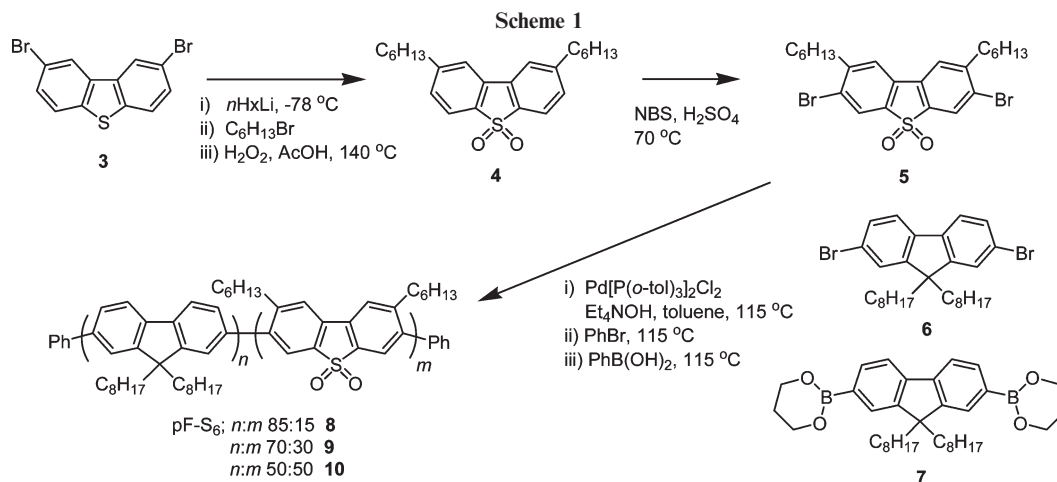

PFO **1**

pF-S copolymers; *n:m* 70:30 = pF-S30 **2**

We have now incorporated new 2,8-dihexyldibenzothiophene-*S,S*-dioxide-3,7-diyl units (S_6 units) into the polyfluorene backbone. Our rationale was twofold: (i) the hexyl chains on the S_6 units should increase the dihedral angles in the polymer backbone, thereby interrupting the extended π-conjugation and blue-shifting the emission; (ii) the solubility of the polymers in common organic solvents should be improved which will facilitate better solution processing, such as spin-coating. Our previous work had shown that copolymers **2** with S unit content >30% produced amorphous insoluble materials. Herein, we report the regiorandom copolymers **8** and **9** and the alternating copolymer **10** and explore the photophysical properties arising from the presence of the S_6 units.

Results and Discussion

Synthesis and Characterization. The synthetic route to monomer unit **5** and the copolymers **8–10** is outlined in Scheme 1. 2,8-Dibromodibenzothiophene[9] underwent halogen–lithium exchange with *n*-hexyllithium and subsequent quenching with *n*-bromohexane to yield the dihexylated product which was oxidized *in situ* with refluxing hydrogen peroxide in acetic acid to give sulfone derivative **4** (50% yield). Compound **4** was then brominated with *N*-bromosuccinimide (NBS) (2.3 equiv) in sulfuric acid. It was noted

*Corresponding author. E-mail: m.r.bryce@durham.ac.uk.

© 2010 American Chemical Society

Published on Web 04/29/2010

pubs.acs.org/Macromolecules

Scheme 1

Table 1. Properties of the Polymers

polymer	feed ratio F:S or S_6	NMR ratio F:S or S_6	M_n/Da	M_w/Da
PFO 1	100:0	100:0	30 734	159 297
pF-S30 2	70:30	72:28	9 855	23 677
8	85:15	85:15	21 390	58 481
9	70:30	67:33	11 191	29 849
10	50:50	55:45	6 597	14 791

that the reaction did not go to completion, and the mono-brominated product was also obtained alongside the desired product **5** (19% yield) during purification. However, addition of further NBS resulted in over-brominated byproducts.

The pF-S_6 copolymers **8−10** were synthesized by Suzuki polycondensation of **5** with 2,7-dibromo-9,9-dioctylfluorene (**6**) and 9,9-dioctylfluorene-2,7-diboronic acid bis(1,3-pro-panediol) (**7**) in toluene with tetraethylammonium hydroxide as an emulsifying base, followed by end-capping with phenyl groups. Bis(tri-o-tolylphosphine)palladium dichloride was chosen as the catalyst due to its higher stability compared to tetrakis(triphenylphosphine)palladium. The polymers **8−10** were obtained with 15%, 30%, and 50% S_6 content, respectively. ^{1}H NMR spectroscopic analysis of the polymers was in good agreement with the feed ratios of the monomers (Table 1 and Figure S1 in the Supporting Information). There are reviews of Suzuki polycondensation reactions which cover the selection of optimal catalyst, solvent, and reaction conditions.[10] We reiterate the importance of thorough purification and accurate stoichiometry of the monomers and a high underlying reaction yield. While the fluorene monomers **6** and **7** could readily be purified to >99% purity (by HPLC analysis) due to their crystalline nature, the monomer **5** retained a small amount of impurity even after repeated recrystallizations. This impurity accounts for the sequential decrease in the molecular weights of the copolymers **8−10** as the ratio of **5** was increased (Table 1). As the molecular weight decreased (increasing S_6 content), the polymers became more powdery compared to the fibers obtained for the higher molecular weight materials. The molecular weights were estimated by GPC analysis compared with a polystyrene standard. The molecular weight of **1** synthesized in our laboratory increased with increased reaction time. In this study, for comparative purposes, we chose polymer **1** obtained after 2 h refluxing as it displayed the closest M_n value to the other polymers. The synthesis of **1** is reported in the Supporting Information. It is notable that whereas polymers **1** and **2** are pale yellow in appearance, polymers **8−10** become whiter in appearance

with increasing ratio of S_6 units in the backbone. The S_6 units considerably increase the solubility compared to analogous pF-S copolymers with the same ratios of F and S subunits (e.g., **9** and **2**).

Photophysical Studies. The pF-S_6 copolymers **8−10** were compared with PFO **1** and copolymer **2**, $n = 0.7$, $m = 0.3$.[8b] All the polymers were end-capped with phenyl units. The data are summarized in Table 2. PFO **1** has bright blue emission that undergoes a small red shift in polar solvents. By incorporating S units in copolymer **2**, the fluorescence in polar solvents, where the ICT state predominates, is significantly red-shifted compared with the emission in nonpolar solvents, where the local exciton (LE) state predominates.[8b] The triplet energy is also increased as a result of the addition of the S units. We now focus on (i) the effects of incorporating S_6 units in **8−10** compared with the original S unit in **2** and (ii) the effects of changing the ratio of S_6 units upon the absorption and emission spectra, the photoluminescence quantum yields (PLQY)s, and triplet energies of copolymers **8−10**.

Two initial general conclusions can be drawn from the addition of the S_6 units into the copolymers: (i) the presence of the S_6 units has a marked effect on the formation of the ICT state; (ii) the hexyl chains of the S_6 unit effectively reduces the conjugation as a result of increased dihedral angles along the backbone. A comparison of **2** and **9** (both polymers with F:S/S_6 ratios of 70:30) can be seen in Figure 1 and Table 2. The alkyl chains of **9** not only blue shift the emission, indicative of conjugation length shortening, but also inhibit the formation of the ICT state in the more polar solvent. By forcing the copolymer **9** to remain twisted, the ICT state is limited in solution, seen as only a small broadening of the spectral peaks. These data suggest that the ICT state in F−S copolymers (with a low ratio of S units) is stabilized by a planar (PICT) (or near-planar) conformation. The limited extent of ICT in the copolymer **9** is also reflected in the increased quantum yield measurements in films (Table 2). Copolymer **9** has a quantum yield in films Φ_{PL} 0.21 which is comparable to PFO **1** (Φ_{PL} 0.16), whereas pF-S30 **2** which is subject to nonradiative decay routes as a result of the prevalent ICT state has a much lower quantum yield (Φ_{PL} 0.07).

The increased solubility due to alkylation of the S unit has enabled the synthesis of pF-S_6 copolymers with a higher content of dibenzothiophene-S,S-dioxide-3,7-diyl units than is the case for copolymers **2**. Table 2 presents the spectral data, PLQYs, and triplet energies of four sulfone-containing copolymers. Figure 2 illustrates the change in spectra as the

Table 2. Photophysical Data for the Polymers

polymer	solvent/film	λ_{max}^{abs}/nm	λ_{max}^{PL}/nm	PLQY, Φ_{PL}	E_T^{onset}/eV^f	E_T^{peak}/eV^f
1	PhMe	382	415 (439)	0.66 ± 0.05^a		
	CHCl$_3$	390	417 (441)			
	film	386	427 (440)	0.16 ± 0.05^b	2.15	2.09
2	PhMe	382	427	0.56 ± 0.05^a		
	CHCl$_3$	384	443			
	film	383	469	0.07 ± 0.05^b	2.19	2.13
8	PhMe	375	413 (437)	0.78 ± 0.05^a		
	CHCl$_3$	380	413 (437)			
	film	377	429 (445)	0.23 ± 0.05^a	2.24	2.17
9	PhMe	359	412 (434)	0.70 ± 0.05^c		
	CHCl$_3$	352	412 (434)			
	film	363	426 (445)	0.21 ± 0.05^d	2.30	2.19
10	PhMe	345	401 (416)	0.70 ± 0.05^c		
	CHCl$_3$	333	414			
	film	350	420	0.50 ± 0.10^e	2.46	2.27

^{a} Excitation wavelength 380 nm. ^{b} Excitation wavelength 390 nm. ^{c} Excitation wavelength 360 nm. ^{d} Excitation wavelength 370 nm. ^{e} Excitation wavelength 350 nm; because of the blue-shifted absorbance of **10**, the excitation wavelength was such that the correction factor of the integrating sphere gives rise to a greater error for **10** compared to the other polymers. ^{f} E_T is the triplet energy.
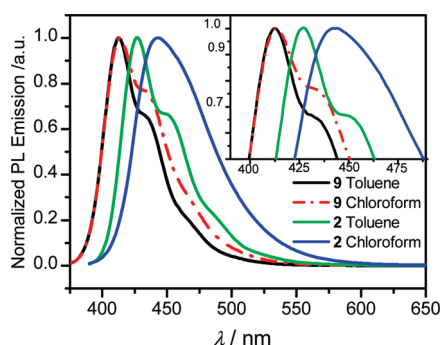

Figure 1. Normalized PL emission spectra of **2** and **9** in toluene and chloroform. Inset shows a magnification of the λ_{max} region.

Figure 2. Normalized PL emission spectra of the copolymers **2**, **8**, **9**, and **10** in chloroform solution. The inset shows the peaks of the normalized emission in toluene (symbols) and chloroform (no symbols). Note for **10** (F:S$_6$ ratio 50:50) the deep-blue emission in toluene and the red shift and broadening in chloroform.

Figure 3. Variable temperature PL emission spectra of **10** in THF (absorption at 340 nm = 0.1 OD) (290−100 K).

ratio of the S$_6$ unit increases (**8** → **9** → **10**) and the behavior of the copolymers in nonpolar (toluene) and polar (chloroform) solution.

The presence of the S$_6$ unit, in any ratio, interrupts the conjugation compared to the homopolymer PFO **1**, such that at an F:S$_6$ ratio of 50:50 (alternating copolymer **10**) each F unit is adjoined by two S$_6$ units. As mentioned above, the hexyl chains on the S$_6$ units restrict the ability of the polymer to adopt a planar conformation. A consequence of this is that the absorption maxima in solution, shown in Table 2, show an incremental blue shift with increasing S$_6$ incorporation as a direct result of reducing the conjugation. The fluorescence spectra in toluene (inset of Figure 2 and Table 2) show only a significant change of λ_{max} for the copolymer **10** which has the highest ratio of S$_6$ units (F:S$_6$ ratio 50:50). The spectrum for **10** is blue-shifted by 11−12 nm compared to **8** and **9**. In the other pF-S$_6$ polymers **8** and **9**, very little solvatochromism is observed as the multiple consecutive fluorene units provide blocks of effectively PFO that are long enough between S$_6$ units that the latter units do not strongly affect the photophysics. The spectra from these copolymers retain sharp well-defined vibronic features in toluene.

In contrast, copolymer **10** in toluene has a broad emission with a slight vibronic shoulder at 416 nm (Figure 2, inset). However, in the more polar chloroform, the emission is further broadened and red-shifted, characteristic of an ICT state. This interpretation was supported by variable temperature measurements in tetrahydrofuran. As the temperature was reduced from 290 to 100 K, enhanced emission was observed from the more-structured, blue-shifted LE state, consistent with freezing out the molecular torsions and
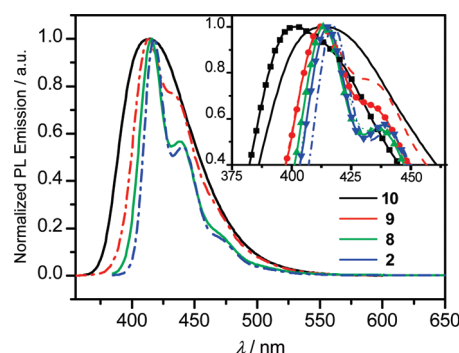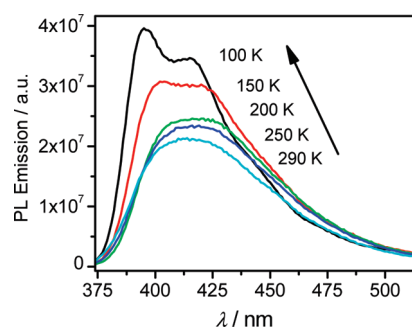
dipole−dipole interactions which stabilize the ICT state (Figure 3).

In chloroform, the presence of the S$_6$ unit in percentages of 15% and 30% (**8** and **9**) has the effect of only broadening the fluorescence spectra. The emission remains centered at λ_{max} 412/413 nm and resembles the emission of PFO **1** (λ_{max} 417 nm). The secondary vibronic shoulder is less well-defined and in a higher ratio to the higher energy peak. The ICT state is presumed essentially absent in the polymers **8** and **9** with the lower ratios of S$_6$ units as a result of steric hindrance (in contrast to pF-S polymers **2** with comparable ratios of S units). However, in the 50:50 copolymer **10** the alternating F and S$_6$ units give rise to strong ICT.

The absorbance in films of PFO **1** occurs at $\lambda_{\max}$ 386 nm, and as the percentage of S_6 unit in the copolymers is increased (**8** → **9** → **10**), the absorbance peak of the films sequentially shifts to the blue (by 9, 23, and 36 nm, relative to PFO), as observed in the solution spectra. The fluorescence is affected by reabsorption which gives the appearance of violating the mirror rule in PFO. The fluorescence from PFO **1** is structured; the main 0−0 transition is at 440 nm, representing a Stokes shift of 35 nm. Copolymers **8** and **9** have a structured emission in films, whereas the 50:50 copolymer **10** has a broad featureless fluorescence spectrum and an increased Stokes shift (70 nm), arising from the ICT state. The addition of the S_6 units increases the PLQY values in thin films compared to pF-S30 **2** (Table 2). The 50:50 copolymer **10** has the highest quantum yield (0.50 ± 0.10) in this series.

Increasing the ratio of the sulfone units, even in small percentages, most significantly affects the triplet energy. For pF-S30 **2** the triplet energy increases slightly compared to PFO **1**, and the S_6 unit further enhances this effect. As the percentage of S_6 increases (**8** → **9** → **10**), the triplet energy increases dramatically to E_T 2.46 eV (onset of phosphorescence) for **10** (Figure 4). This is due to the shorter conjugation lengths which result from enhanced twisting of the backbone.

Earlier work has shown the inverse relationship between triplet energy and conjugation length in twisted polythiophenes.[11] It is known that conjugated polymers with low-lying triplet levels are unsuitable host materials as they quench the triplet exciton of guest species by back-transfer of energy, leading to low PL and EL efficiencies.[12] PFO **1** has a relatively low triplet energy (E_T ca. 2.1−2.2 eV) which limits its use as a host material. PFO **1** is, therefore, an effective host polymer only for red-emitting complexes without back-transfer of energy from the dopant to the host.[13] Unless additional interlayers are added which complicate the device architecture (e.g., polyvinylcarbazole as an anode buffer layer),[14] PFO is unsuitable as a host for green, blue,

and three-color (RGB) white-emitting devices based on phosphorescent emitters.[15] Polymer **10** with its high triplet energy is, therefore, a prime candidate for hosting green phosphorescent materials, and we now discuss this aspect of the work.

Electroluminescence Properties of PLEDs. Initial electroluminscence measurements have been carried out. Devices were prepared with the following structures: glass/ITO (150 nm)/PEDOT:PSS (50 nm)/LEP/Ba (4 nm)/Al (100 nm). Data are collated in Table 3. Devices 1 and 2 were made from **10**, either pure or as a blend containing the soluble green-emitting iridium complex **11**[16] (Chart 2). Devices 3−5 were made from polymers **8**, **9**, and **10**, all blended with **11**. The aim was a comparative study to investigate how the ratio of S_6 units (and thus the triplet energy) affected these polymers' suitability as hosts for **11**. Device data are summarized in Table 3. $J−V−B$ curves for the devices are shown in the Supporting Information.

Device 1 showed deep blue emission from the pure polymer **10**, with CIE coordinates (0.18, 0.15). Device 2 showed emission only from the green guest complex **11** (0.35, 0.62) (Figure 5). The slightly reduced current density in device 2 provides tentative evidence that charge trapping on the guest takes place, providing one route to the formation of excitations there. Additionally, triplet exciton transfer from the host polymer **10** may occur. Despite the reduced current density, device 2 exhibited higher brightness values than

Figure 5. Electroluminescence spectra from devices 1 (blue line) and 2 (green line) at current densities of ca. 7 mA cm^{-2}.
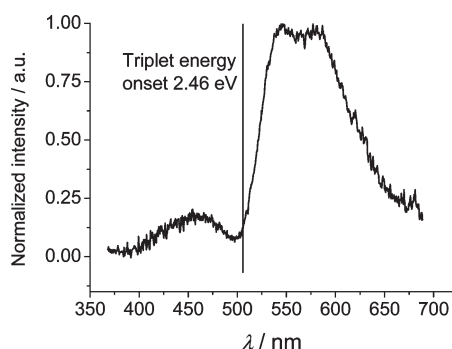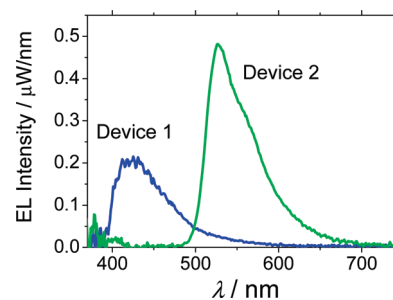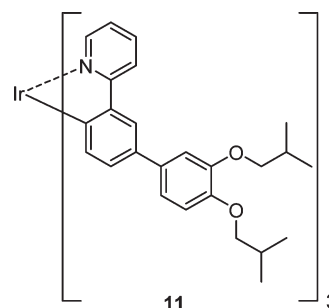
Chart 2

Figure 4. Normalized phosphorescence and delayed emission of a spun film of **10** (delay 205 ms and integration time = 50 ms). The triplet energy at the onset is marked on the spectrum.

Table 3. Electroluminescent Device Data

device no.	LEP (thickness)	$V_{\text{turn-on}}$/V[a]	V_{comp}/V	J_{comp}/ mA cm^{-2}	B/cd m^{-2}	current efficacy/cd A^{-1}	efficacy/ lm W^{-1}	EQE/%	CIE (x, y)[b]
1	**10** (65 nm)	4.9	9.0	36	85	0.24	0.08	0.2	0.18, 0.15
2	**10** + 10% w/w **11** (65 nm)	4.1	7.4	1.9	102	5.5	2.3	1.5	0.35, 0.62
3	**8** + 3.3% w/w **11** (50 nm)	4.0	7.0	94	95	0.10	0.05	0.06	0.23, 0.29
4	**9** + 3.3% w/w **11** (50 nm)	5.0	8.0	32	78	0.24	0.10	0.1	0.29, 0.44
5	**10** + 3.3% w/w **11** (50 nm)	4.9	8.0	18	93	0.52	0.20	0.17	0.33, 0.58

[a] Turn-on voltage is defined here as the voltage at which device brightness reached 1 cd m^{-2}. For comparison, devices were all measured at an applied voltage V_{comp} (with current density J_{comp}) at which the device brightness B was as close as possible to 100 cd m^{-2} over the measurement range. [b] A CIE diagram is shown in the Supporting Information (Figure S10).

device 1. The phosphorescent nature of the guest provides higher quantum efficiencies and additionally shifts the emission from blue to green, where the human eye is more sensitive. Electroluminescence spectra from these devices 3−5 are shown in Figure 6.

The devices exhibit low turn-on voltages and efficiencies of up to 5.5 cd A^{-1} and EQE 1.5%. It should be noted that these efficiencies consider only light emitted through the substrate; light waveguided from the edges was not recorded. These are unoptimized devices and performance might be improved by inserting additional layers to improve charge balance. However, we have not explored this aspect as our aim is to retain as simple a device structure as possible.

To provide additional information on the energy transfer mechanisms in these blends, photoluminescence measurements were made on devices 3−5 before the devices had been operated electrically. The results are shown in Figure 7. The
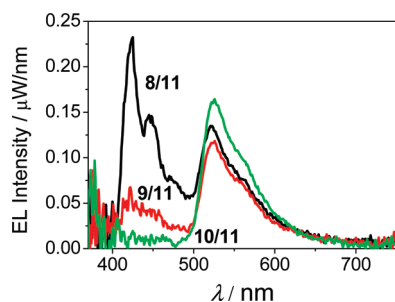

Figure 6. Electroluminescence spectra from devices 3 (black line), 4 (red line), and 5 (green line) comprising blends of **8**, **9**, and **10** with **11** (3.3% w/w), respectively. These spectra correspond to brightnesses of ca. 100 cd m^{-2}.
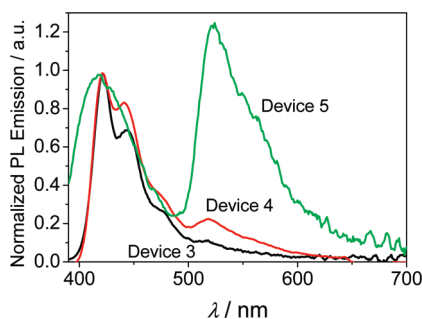

Figure 7. Normalized PL measurements on devices 3 (black line), 4 (red line), and 5 (green line). Excitation was at 370 nm.

ratio of green to blue emission is reduced relative to the EL measurements. Indeed, blue fluorescence from the host polymer was observed from all the materials (**8**, **9**, and **10**), whereas in EL measurements emission from **10** was absent. This provides additional evidence that under electrical operation excitons are formed on the guest **11** by direct charge trapping, as was suggested to occur in device 2. Although Dexter energy transfer of triplet excitons cannot be ruled out, this would not reduce the fluorescence from the host polymer.

Whatever mechanism is operating, if the triplet energy of the guest is higher than that of the host, then green emission from the phosphorescent guest will be reduced. Dexter transfer to the guest will be unlikely, and any excitons forming on the guest by direct charge trapping may transfer to the lower energy triplet on the host polymer. In this series of devices, emission from the phosphorescent guest becomes more intense as the amount of S$_6$ in the host polymer increases. It is clear that the higher triplet energy is preventing energy transfer to the host. The results show convincingly that these polymers, **10** in particular, can serve as hosts for green phosphorescent materials.

To place our work in context, we now briefly summarize the literature data for conjugated polymers that are capable of hosting green phosphorescent dopants (Chart 3). The alternating copolymer **12** with *meta* linkages in the backbone to shorten the conjugation length has a triplet energy E_T 2.56 eV (λ_{max} of the emission in the phosphorescence spectrum) and is a host for the guest complex **11** with emission only from **11**. However, only limited characterization data were reported for polymer **12**, and the structure of the side chains R was not disclosed.[17] An analogous polymer, with a 2,5-diaryl-1,3,4-oxadiazole unit pendant from one of the carbazole units, showed E_T 2.52 eV (λ_{max} of the emission), but no devices with green dopants were reported.[18] Poly(3,6-dibenzosilole), **13**, which shows onset of the triplet emission at 2.55 eV was successfully doped with the green-emitting triplet complex Ir(m-ppy)$_3$ with no emission from the host. However, the efficiency and brightness data were not reported.[19] Poly(3,6-fluorene), **14** (E_T 2.58 eV for λ_{max} of the emission), was doped with the sky-blue-emitting Ir complex (FIrpic) to give mixed emission from both host and dopant.[20] A device comprising polymer **15** and a green-emitting guest complex, with an interlayer of PVK, showed a high turn-on voltage and no host emission. The triplet level of **15** was not reported.[21] Polymer **16** (E_T 2.60 eV for λ_{max} of the emission) hosted the green emitter Ir(ppy)$_3$, and devices using an evaporated hole blocking/exciton confinement

Chart 3
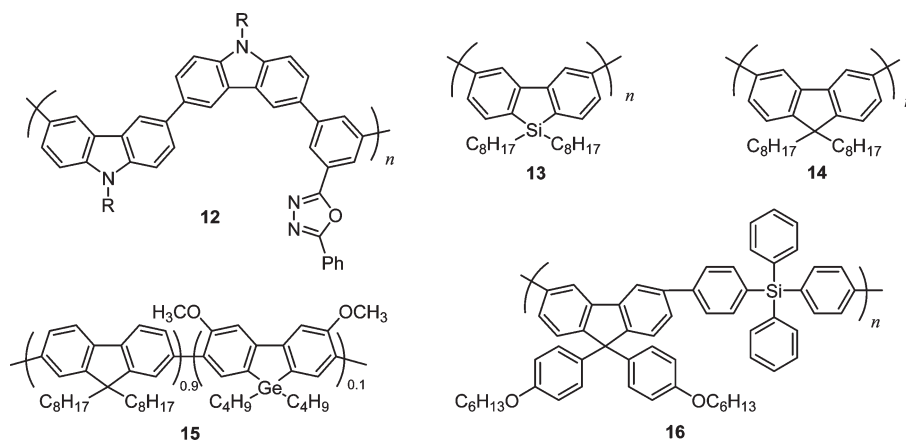
layer showed emission only from the dopant.[22] The new polymer **10**, therefore, competes favorably with those reported in the literature as a host for green phosphors.

Conclusions

New donor−acceptor fluorene-based copolymers have been studied. 2,8-Dihexyldibenzothiophene-*S*,*S*-dioxide-3,7-diyl units have been incorporated into copolymers (pF-S$_6$ **8**−**10**) by Suzuki− Miyaura polymerization. The hexyl substituents on the S$_6$ moieties exert a profound effect on the properties of the copolymers. Solubility in common organic solvents is improved, and conjugation is reduced due to enhanced dihedral angles in the backbone. The emission is shifted deep into the blue (λ_{max} 420 nm for films of **10**). At lower ratios of S$_6$ units (15% and 30%) the backbone twist limits the ICT emission as a consequence of reduced donor−acceptor interactions between the F and S$_6$ units. However, this effect is overcome in the 50:50 copolymer **10** by increased interaction between adjacent F and S$_6$ units and strong ICT emission is observed. The triplet energy is raised significantly compared to conventional fluorene copolymers and increases as the percentage of the S$_6$ unit increases (i.e., 15%, 30%, 50%: **8** → **9** → **10**). It has been established that the alternating copolymer **10** (E_T 2.46 eV for onset of phosphorescence) is a suitable host for a green phosphorescent iridium guest emitter. Electroluminescence device studies using a blend of **10** and a soluble Ir(ppy)$_3$ derivative showed emission only from the guest complex.

Experimental Section

Materials and Measurements. Materials obtained from commercial suppliers were used without further purification. Solvents were dried and degassed following standard procedures. ^{1}H NMR and ^{13}C NMR spectra were recorded on Bruker Avance 400 or Varian VNMRS 700 spectrometers with TMS as an internal standard. Mass spectra were measured on a Waters Xevo OTofMS with an ASAP probe. Elemental analysis was performed on a CE-400 elemental analyzer. HPLC analysis was carried out using a PerkinElmer Series 200 HPLC instrument equipped with a diode array detector, usually monitoring at 254 nm. The column was a Phenomenex HyperClone 5 μm ODS (C18) 120 Å, 250 × 4.6 mm; flow rate 1 mL min^{-1}. Gel permeation chromatography was carried out on a Viscotek TDA 302 with refractive index, viscosity, and light scattering detectors and 2 × 300 mL PLgel 5 μm mixed C columns; THF was used as the eluent at a flow rate of 1.0 mL min^{-1} and at a constant temperature of 35 °C. Samples were analyzed using a conventional calibration generated with a series of narrow polydispersity polystyrene standards (192−1 111 200 g mol^{-1}) obtained from Polymer Laboratories. 2,7-Dibromo-9,9-dioctyl-fluorene (**6**),[23] 9,9-dioctylfluorene-2,7-diboronic acid bis(1,3-propanediol) ester (**7**),[23] and the iridium complex **11**[16] were synthesized according to published procedures. The monomers were purified by recrystallization from ethanol and then hexane (**6**) and acetonitrile and then hexane (**7**).

Solution and solid state absorption and emission spectra were obtained using a Shimadzu UV−vis−NIR spectrophotometer and a Jobin-Yvon fluoromax spectrofluorimeter, respectively. Solid state photoluminescence quantum yields were taken using a calibrated Labsphere integrating sphere held within the spectrofluorimeter. Excitation wavelengths corresponded to the maximum absorbance of the polymer under investigation. The triplet energy of a film at a temperature of 17 K was calculated from a gated luminescent measurement of the phosphorescence. The equipment is described in detail elsewhere.[24] Solutions, in toluene or chloroform, were kept below 0.1 OD. Solid state samples were spun-cast films, cast from a toluene solution of 10 mg mL^{-1}, and had a maximum absorbance of 2.0 OD.

Sheets of polished glass coated with indium tin oxide (ITO) with a sheet resistance of 15 ohm sq^{-1} were purchased from Visiontek. The sheets were cut into substrates of dimensions 24 mm × 24 mm. The ITO was patterned via photolithography to give two stripes 5 mm wide. The substrates were cleaned via ultrasonication in detergent, deionized water, acetone, and isopropanol, followed by 10 min UV ozone treatment. The polymer layers were formed by spin-coating from solution. The PEDOT:PSS used was Clevios AI4083, purchased from HC Starck. The light-emitting polymers were dissolved in xylene at a concentration of 15 mg mL^{-1}. Prior to deposition, all solutions were filtered using 0.45 μm PVDF filters. After deposition of the PEDOT:PSS layer, the substrates were baked at 150 °C in air. They were then transferred to a nitrogen glovebox where the light-emitting polymer layers were spin-coated. Barium was used as the cathode material and capped with aluminum. These layers were deposited via thermal evaporation through a shadow mask at a pressure of 1×10^{-6} mbar. Two stripes, 4 mm wide and perpendicular to the ITO stripes, were formed, creating four devices of dimensions 4 × 5 mm. Finally, the devices were encapsulated with a glass plate held in place with a UV-curable epoxy resin (DELO).

Devices were characterized inside a 10-in. LabSphere integrating sphere. Power was supplied by an Agilent 6632B dc power supply. Electroluminescence spectra were recorded by an Ocean Optics USB4000 CCD spectrometer, connected to the sphere by an optical fiber. The system was calibrated so that the absolute optical power output of the devices could be measured. Devices were mounted in a sample holder such that only light emitted through the substrate surface could be detected; i.e., no waveguided light through the edges of the devices contributed to the emission. Voltages were swept with the current and electroluminescence spectra measured at each point.

2,8-Dihexyldibenzothiophene-*S*,*S*-dioxide (4). An argon-purged flask was charged with **3**[9] (10.0 g, 29.3 mmol) and THF (200 mL), and the solution was cooled to −78 °C. A solution of *n*-hexyllithium was added dropwise (28 mL, 2.3 M, 64.4 mmol), and the yellow solution was stirred for 3 h. *n*-Hexyl bromide (10.0 mL, 71.2 mmol) was added, and the solution was allowed to warm to room temperature. Water was added, and the solution was stirred for 2 h. Diethyl ether was added, and the layers were separated. The aqueous layer was extracted with more diethyl ether, and the combined organic layers were washed with water, dried (MgSO$_4$), filtered, and concentrated to yield a yellow oil. The oil was dissolved in acetic acid (50 mL), and hydrogen peroxide (30% w/w in water) (15 mL) was carefully added; the solution was heated with stirring at 140 °C for 2 h, then more hydrogen peroxide was added (10 mL), and the solution was heated for an additional 16 h. After cooling, water (150 mL) was added, and the product was extracted with chloroform, washed with water, dried (MgSO$_4$), filtered, and concentrated to yield a yellow oil which was recrystallized from ethanol in the freezer to yield a white solid (5.60 g, 50%); mp 74.9−76.1 °C. δ_H (400 MHz, CDCl$_3$): 7.68 (d, *J* 7.9 Hz, 2H), 7.56 (d, *J* 0.9 Hz, 2H), 7.29 (dd, *J* 7.9, 1.4 Hz, 2H), 2.77−2.60 (m, 4H), 1.72−1.59 (m, 4H), 1.45−1.24 (m, 12H), 0.88 (dd, *J* 8.9, 5.2 Hz, 6H). δ_C (101 MHz, CDCl$_3$): 149.9, 136.0, 132.3, 130.6, 122.2, 121.5, 36.5, 31.9, 31.4, 29.1, 22.8, 14.3. ν_{max} (film)/ cm^{-1}: 2925 (C−H), 2855 (C−H), 1604 (Ar C−H), 1286 (S=O), 1127 (S=O), 1175, 1152. λ_{max} (MeCN): 240, 248 nm (ε 162 280, 159 280 cm^{-1} mol^{-1} dm^3); MS-APCI+ *m/z* 384.2 ([M$^+$], 100%). HRMS-ACPI+ [M$^+$ + H] calcd: 385.2201; found: 385.2210. Anal. Calcd for C$_{24}$H$_{32}$O$_2$S: C, 74.95; H, 8.39. Found: C, 74.49; H, 8.20.

3,7-Dibromo-2,8-dihexyldibenzothiophene-*S*,*S*-dioxide (5). An argon-purged flask was charged with 2,8-dihexyldibenzothiophene-*S*,*S*-dioxide, **4** (5.00 g, 13.0 mmol), and sulfuric acid (300 mL). The mixture was heated to 70 °C in the dark, and *N*-bromosuccinimide (NBS) (5.20 g, 29.2 mmol) was added in portions. After stirring for 24 h TLC analysis showed the presence of both monobrominated and dibrominated materials so a further portion

of NBS (1.00 g, 5.6 mmol) was added and stirring continued for 16 h. Water was added (CAUTION: exothermic reaction), and the organics were extracted with chloroform, washed with brine, dried (MgSO$_4$), filtered, and concentrated to yield a yellow oil. The oil was chromatographed on a silica column eluting with petrol ether bp 40−60:DCM 1:1 v/v. Both the monobromo and dibromo products were isolated (255 mg, 4%) and (1.32 g, 19%), respectively, as white solids which could be recrystallized from ethanol. Compound **5**: mp 167.9−169.2 °C. δ_H (400 MHz, CDCl$_3$): 7.91 (s, 2H), 7.56 (s, 2H), 2.85−2.74 (m, 4H), 1.74−1.57 (m, 4H), 1.47−1.26 (m, 12H), 0.89 (dd, *J* 9.5, 4.7 Hz, 6H). δ_C (101 MHz, CDCl$_3$): 149.2, 136.8, 130.5, 126.8, 126.4, 122.8, 77.6, 77.2, 76.9, 37.1, 31.8, 29.9, 29.3, 22.8, 14.3. MS-APCI+ *m/z* 542.0 ([M$^+$], 100%). HRMS-APCI+ [M$^+$ + H] calcd: 541.0411; found: 541.0394. Data for the monobrominated compound are as follows: mp 112.9−114.1 °C. δ_H (400 MHz, CDCl$_3$): 7.92 (s, 1H), 7.67 (d, *J* 7.9 Hz, 1H), 7.60−7.52 (m, 2H), 7.31 (dd, *J* 7.9, 1.4 Hz, 1H), 2.88−2.75 (m, 2H), 2.75−2.65 (m, 2H), 1.73−1.57 (m, 4H), 1.49−1.19 (m, 12H), 0.98−0.76 (m, 6H). ^{13}C NMR (101 MHz, CDCl$_3$): δ 150.27, 148.82, 137.20, 135.54, 131.47, 131.26, 130.85, 126.63, 125.99, 122.90, 122.32, 121.54, 37.04, 36.47, 31.83, 31.79, 31.40, 29.88, 29.28, 29.07, 22.78, 22.77, 14.28, 14.27. MS-APCI+ *m/z* 463.12 ([M + H]$^+$, 100%). HRMS-APCI+ [M$^+$] calcd: 462.1228; found: 462.1227. Anal. Calcd for C$_{24}$H$_{31}$BrO$_2$S: C, 62.20; H, 6.74. Found: C, 61.92; H, 6.67.

Polymerization Reactions. *pF-S$_6$ Copolymer* (**8**) (*F:S$_6$ Ratio 85:15*). A flask was charged with 9,9-dioctylfluorene-2,7-diboronic acid bis(1,3-propanediol) ester, **7** (400.0 mg, 0.713 mmol, purity 99.5%), 2,7-dibromo-9,9-dioctylfluorene, **6** (275.0 mg, 0.501 mmol, purity 99.9%), 3,7-dibromo-2,8-dihexyldibenzothiophene-S,S-dioxide, **5** (117.5 mg, 0.214 mmol, purity 99%), and toluene (16 mL). The mixture was degassed for 15 min before bis[(tri-*o*-tolyl)phosphine]palladium dichloride (11 mg, 1 mol %) was added, and degassing continued for 15 min before a degassed 20 wt % solution of tetraethylammonium hydroxide in water (4 mL) was added, and the mixture was vigorously stirred at 115 °C with protection from light for 18 h. Bromobenzene (0.1 mL) was added, stirring was continued at 115 °C for 1 h before benzeneboronic acid (100 mg) was added, and stirring continued at 115 °C for 1 h. After cooling, the gray mixture was added slowly to stirring methanol (300 mL) to precipitate the crude polymer as gray fibers. The fibers were filtered and washed sequentially with methanol, water, and methanol. The polymer was redissolved in toluene (20 mL), an aqueous solution of *N,N*-diethyldithiocarbamic acid sodium salt (ca. 0.5 M, 15 mL) was added, and the mixture was stirred at 65 °C for 16 h. The layers were separated, and the aqueous layer was extracted with toluene. The combined organic layers were washed with dilute HCl solution, sodium acetate solution, and twice with water before being passed through a Celite 545 plug to yield a clear yellow solution. The solution was concentrated until it became viscous and was then added dropwise to stirring methanol (350 mL) to precipitate the polymer as off-white fibers which were isolated by filtration and washed with methanol and acetone to give **12** (503 mg, 91%). δ_H (400 MHz, CDCl$_3$): 7.77 (m), 7.32 (br), 2.77 (br), 2.13 (br), 1.33−1.00 (m), 0.80 (m).

pF-S$_6$ Copolymer (**9**) (*F:S$_6$ Ratio 70:30*). Following the procedure for **8**, compounds **7** (344.0 mg, 0.612 mmol, purity 99.5%), **6** (135.0 mg, 0.246 mmol, purity 99.9%), and **5** (200.0 mg, 0.364 mmol, purity 99%) yielded **9** as white fibers (420 mg, 90%). δ_H (400 MHz, CDCl$_3$): 7.74 (m), 7.31 (s), 2.76 (br), 2.03 (br), 1.16 (m), 0.87−0.50 (m).

pF-S$_6$ Copolymer (**10**) (*F:S$_6$ Ratio 50:50*). Following the procedure for **8**, compounds **7** (306.5 mg, 0.546 mmol, purity 99.5%) and **5** (300.0 mg, 0.546 mmol, 99% purity) gave **10** as a white powder (390 mg, 93%). δ_H (400 MHz, CDCl$_3$): 7.85−7.71 (m), 7.32 (m), 2.74 (br), 2.00 (br), 1.28−0.97 (m), 0.79 (m).

Supporting Information Available: Synthesis of PFO **1**; additional absorption and emission spectra; CIE diagram for devices 1−5; *J*−*V*−*B* curves for the devices; copy of the ^{1}H NMR spectrum of polymer **8**. This material is available free of charge via the Internet at http://pubs.acs.org.

References and Notes

(1) *Polyfluorenes*; Adv. Polym. Sci. 212; Scherf, U., Neher, D., Eds.; Springer-Verlag: Berlin, 2008.

(2) (a) Scherf, U.; List, E. J. W. *Adv. Mater.* **2002**, *14*, 477−487. (b) Leclerc, M. *J. Polym. Sci., Part A: Polym. Chem.* **2001**, *39*, 2867−2873.

(3) Fomina, N.; Bradforth, S. E.; Hogen-Esch, T. E. *Macromolecules* **2009**, *42*, 6440−6447.

(4) (a) Beaupré, S.; Leclerc, M. *Adv. Funct. Mater.* **2002**, *12*, 192−196. (b) Yang, R.; Tian, R.; Yan, J.; Zhang, Y.; Yang, J.; Hou, Q.; Yang, W.; Zhang, C.; Cao, Y. *Macromolecules* **2005**, *38*, 244−253. (c) Wu, W.-C.; Liu, C.-L.; Chen, W.-C. *Polymer* **2006**, *47*, 527−538. (d) Zhu, Y.; Gibbons, K. M.; Kulkarni, A. P.; Jenekhe, S. A. *Macromolecules* **2007**, *40*, 804−813. (e) Kulkani, A. P.; Zhu, Y.; Jenekhe, S. A. *Macromolecules* **2008**, *41*, 339−345. (f) Wu, P.-T.; Kim, F. S.; Champion, R. D.; Jenekhe, S. A. *Macromolecules* **2008**, *41*, 7021−7028.

(5) (a) Perepichka, I. I.; Perepichka, I. F.; Bryce, M. R.; Palsson, L.-O. *Chem. Commun.* **2005**, 3397−3399. (b) King, S. M.; Perepichka, I. I.; Perepichka, I. F.; Dias, F. B.; Bryce, M. R.; Monkman, A. P. *Adv. Funct. Mater.* **2009**, *19*, 586−591.

(6) (a) Liu, J.; Zou, J.; Yang, W.; Wu, H.; Li, C.; Zhang, B.; Peng, J.; Cao, Y. *Chem. Mater.* **2008**, *20*, 4499−4506. (b) Li, Y.; Wu, H.; Zou, J.; Ying, L.; Yang, W.; Cao, Y. *Org. Electron.* **2009**, *10*, 901−909. (c) For random poly(fluorenevinylene)s containing 3,7-dibenzothiophene-S,S-dioxide units: Grisorio, R.; Piliego, C.; Cosma, P.; Fini, P.; Mastrorilli, P.; Gigli, G.; Suranna, G. P.; Nobile, C. F. *J. Polym. Sci., Part A: Polym. Chem.* **2009**, *47*, 2093−2104.

(7) (a) Gong, X.; Iyer, P. K.; Moses, D.; Bazan, G. C.; A. J. Heeger, A. J.; Xiao, S. S. *Adv. Funct. Mater.* **2003**, *13*, 325−330. (b) List, E. J. W.; Guentner, R.; de Freitas, P. S.; Scherf, U. *Adv. Mater.* **2002**, *14*, 374−378. (c) Cho, S. Y.; Grimsdale, A. C.; Jones, D. J.; Watkins, S. E.; Holmes, A. B. *J. Am. Chem. Soc.* **2007**, *129*, 11910−11911. (d) Specific substituents at C(9) of fluorene improve spectral stability: McFarlane, S. L.; Piercey, D. G.; Coumont, L. S.; Tucker, R. T.; Fleischauer, M. D.; Brett, M. J.; Veinot, J. G. C. *Macromolecules* **2009**, *42*, 591−598.

(8) (a) Dias, F. B.; Pollock, S.; Hedley, G.; Palsson, L.-O.; Monkman, A.; Perepichka, I. I.; Perepichka, I. F.; Tavasli, M.; Bryce, M. R. *J. Phys. Chem. B* **2006**, *110*, 19329−19339. (b) Dias, F. B.; King, S.; Monkman, A. P.; Perepichka, I. I.; Kryuchkov, M. A.; Perepichka, I. F.; Bryce, M. R. *J. Phys. Chem. B* **2008**, *112*, 6557−6566. (c) Dias, F. B.; Kamtekar, K. T.; Cazati, T.; Williams, G.; Bryce, M. R.; Monkman, A. P. *ChemPhysChem* **2009**, *10*, 2096−2104.

(9) Yang, W.; Hou, Q.; Liu, C.; Niu, Y.; Huang, J.; Yang, R.; Cao, Y. *J. Mater. Chem.* **2003**, *13*, 1351−1355.

(10) (a) Murage, J.; Eddy, J. W.; Zimbalist, J. R.; McIntyre, T. B.; Wagner, Z. R.; Goodson, F. E. *Macromolecules* **2008**, *41*, 7330−7338. (b) Sakamoto, J.; Rehahn, M.; Wegner, G.; Schlüter, A. D. *Macromol. Rapid Commun.* **2009**, *30*, 653−687.

(11) Monkman, A. P.; Burrows, H. D.; Hamblett, I.; Navarathnam, S.; Svensson, M.; Andersson, M. R. *J. Chem. Phys.* **2001**, *115*, 9046−9049.

(12) (a) Chen, F.-C.; He, G.; Yang, Y. *Appl. Phys. Lett.* **2003**, *82*, 1006−1008. (b) Sudhakar, M.; Djurovich, P. I.; Hogen-Esh, T. E.; Thompson, M. E. *J. Am. Chem. Soc.* **2003**, *125*, 7796−7797.

(13) (a) Gong, X.; Ostrowski, J. C.; Bazan, G. G.; Moses, D.; Heeger, A. J.; Liu, M. S.; Jen, A. K. Y. *Adv. Mater.* **2003**, *15*, 45−49. (b) Wang, L.; Liang, B.; Huang, F.; Peng, Y.; Cao, Y. *Appl. Phys. Lett.* **2006**, *89*, 151115.

(14) Chen, Z.; Jiang, C.; Niu, Q.; Peng, J.; Cao, Y. *Org. Electron.* **2008**, *9*, 1002−1009.

(15) WOLED reviews: (a) Kamtekar, K. T.; Monkman, A. P.; Bryce, M. R. *Adv. Mater.* **2010**, *22*, 572−582. (b) D'Andrade, B. W.; Forrest, S. R. *Adv. Mater.* **2004**, *16*, 1585−1595.

(16) Stössel, P.; Bach, I.; Spreitzer, H. WO Pat. WO2004026886, **2004**.

(17) van Dijken, A.; Bastiaansen, J. J. A. M.; Kiggen, N. M. M.; Langeveld, B. M. W.; C. Rothe, C.; Monkman, A.; Bach, I.;

Stössel, P.; Brunner, K. *J. Am. Chem. Soc.* **2004**, *126*, 7718–7727.

(18) Zhang, K.; Tao, Y.; Yang, C.; You, H.; Zou, Y.; Qin, J.; Ma, D. *Chem. Mater.* **2008**, *20*, 7324–7331.

(19) Chan, K. L.; Watkins, S. E.; Mak, C. S. K.; McKiernan, M. J.; Towns, C. R.; Pascu, S. I.; Holmes, A. B. *Chem. Commun.* **2005**, 5766–5768.

(20) Wu, Z.; Xiong, Y.; Zou, J.; Wang, L.; Liu, J.; Chen, Q.; Yang, W.; Peng, J.; Cao, Y. *Adv. Mater.* **2008**, *20*, 2359–2364.

(21) Chen, R.-F.; Zhu, R.; Zheng, C.; Liu, S.-J.; Fan, Q.-L.; Huang, W. *Sci. China, Ser. B: Chem.* **2009**, *52*, 212–218.

(22) Yeh, H.-C.; Chien, C.-H.; Shih, P.-I.; Yuan, M.-C.; Shu, C.-F. *Macromolecules* **2008**, *41*, 3801–3807.

(23) Towns, C. R.; O'Dell, R. WO Pat. WO0055927, **2000**.

(24) (a) Jankus, V.; Winscom, C.; Monkman, A. P. *J. Chem. Phys.* **2009**, *130*, 074501. (b) Rothe, C.; Monkman, A. P. *Phys. Rev. B: Condens. Matter* **2003**, *68*, 075208.